Delft University of Technology

Unparameterized optimization of the spring characteristic of parallel elastic actuators

van der Spaa, Linda F.; Wolfslag, Wouter J.; Wisse, Martijn

DOI
10.1109/LRA.2019.2893425

Publication date
2019

Document Version
Accepted author manuscript

Published in
IEEE Robotics and Automation Letters

Citation (APA)
van der Spaa, L. F., Wolfslag, W. J., & Wisse, M. (2019). Unparameterized optimization of the spring characteristic of parallel elastic actuators. *IEEE Robotics and Automation Letters*, *4*(2), 854-861. https://doi.org/10.1109/LRA.2019.2893425

Important note
To cite this publication, please use the final published version (if applicable).
Please check the document version above.

Copyright
Other than for strictly personal use, it is not permitted to download, forward or distribute the text or part of it, without the consent of the author(s) and/or copyright holder(s), unless the work is under an open content license such as Creative Commons.

Takedown policy
Please contact us and provide details if you believe this document breaches copyrights.
We will remove access to the work immediately and investigate your claim.

This work is downloaded from Delft University of Technology.
For technical reasons the number of authors shown on this cover page is limited to a maximum of 10.

Unparameterized Optimization of the Spring Characteristic of Parallel Elastic Actuators

Linda F. van der Spaa[1], Wouter J. Wolfslag[2], Martijn Wisse[1]

***Abstract*— In electrically actuated robots most energy losses are due to the heating of the actuators. This energy loss can be greatly reduced with parallel elastic actuators, by optimizing the elastic element such that it delivers most of the required torques. Previously used optimization methods relied on parameterizing the spring characteristic, thereby limiting the set of spring characteristics optimized over and with that the loss reduction that can be obtained. This paper shows that such parametrization is not necessary; a method is presented to compute the optimal characteristic as an *analytic* function of the trajectory. The efficacy of this method is demonstrated using two examples. The first example considers the optimal spring characteristic for a parallel elastic actuator supporting the human ankle during walking. The second example applies the method in combination with trajectory optimization on a single degree of freedom robot performing a specific pick-and-place task. The task at hand has a height difference between the pick and the place location. With the analytical optimal spring, it is shown that the robot can recover enough of the energy released by the package to function without external electric energy supply.**

I. Introduction

The main source of energy loss in robots is the heating of their electric actuators [1]. This heating is proportional to the square of the electric current, which in turn is proportional to the required motor torque. The torque requirements on the actuator can be greatly reduced by adding a parallel elastic element. The decrease in torque requirement allows smaller gearbox ratios, thereby decreasing gearbox losses and improving torque control [2]. The use of such parallel elastic actuators is widespread, for examples see the works on robot manipulators [3], [4], robot legs [5] and exoskeletons [2]. Their most generic use as a way of saving energy is observed in static balancing mechanisms [4]–[7], which compensate for gravity such that small actuators are sufficient to power the robot. If the desired motions of the robot are known beforehand, the elastic element can take them into account, thereby providing some of the force required for that motion. This approach has already led to large reductions in energy consumption for different repetitive tasks [3], [5], [8]–[10]. These designs all aim to capture kinetic energy from the robot arm, and release that energy again at appropriate times in the motion. The springs themselves typically perform this recapturing and releasing at an efficiency of over 90%, much higher than what can be reached via electric storage. However, spring mechanism designs so far have not reached the goal of minimum energy consumption. Therefore, this paper considers optimization of the spring characteristic of parallel elastic actuators for minimum energy use.

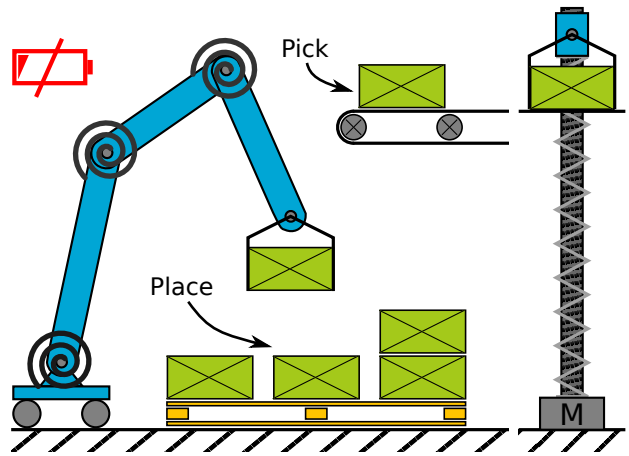

(a) (b)

Fig. 1: Plugless robot arm. **(a)** Explains the idea; the robot performs a pick and place task where the pick position is higher than the place position. With aid of (nonlinear) springs, as illustrated on the joints, the gravitational energy of the package can be recovered to power the robot. **(b)** Shows the simulation model, consisting of a single degree of freedom robot including a motor and transmission model.

Our motivation is the eventual development of a plugless robot arm, see Fig. 1. The pick-and-place task this system performs adds energy to the system by having the pick position be higher than the place position. The energy released from the package can be recovered electrically when allowing the actuator to function as generator. When enough energy can be recovered, the system will be capable of powering the return motion carrying the unloaded arm back to the top position. Then this robot arm will not need an external electric power supply, hence the name plugless arm. Even more energy could be recovered and used to power systems such as on-board microcontrollers and sensors.

This plugless arm is a design challenge aimed at developing and integrating energy saving technologies for robotics [11]. Such energy efficiency is particularly important to increase the uptime of mobile-base robot manipulators. One of the key technologies used will be parallel elastic actuators. Due to the limited amount of energy available, finding the

[1]Linda F. van der Spaa and Martijn Wisse are with the Faculty of Mechanical, Maritime and Materials Engineering (3ME), Department of Cognitive Robotics, Delft University of Technology, 2628 CD Delft, The Netherlands {l.f.vanderspaa, m.wisse}@tudelft.nl

[2]Wouter J. Wolfslag is with the School of Informatics, Institute of Perception, Action and Behaviour, University of Edinburgh, Edinburgh EH8 9AB, U.K. wouter.wolfslag@ed.ac.uk

© 2019 IEEE. Personal use of this material is permitted. Permission from IEEE must be obtained for all other uses, in any current or future media, including reprinting/ republishing this material for advertising or promotional purposes, creating new collective works, for resale or redistribution to servers or lists, or reuse of any copyrighted component of this work in other works.

exact optimal spring characteristic is vital.

The optimization approaches for task specific spring mechanisms in literature can be classified into the following three categories:

1) A linear spring is fit to trajectory data [8], [10]. Peak power is reduced, but the fit becomes poorer as the desired characteristic gets more nonlinear.
2) The parameters of a pre-specified (complex), task-specific mechanism are optimized to fit trajectory data [12], [13].
3) The optimal parameters defining the spring are expressed as a function of the trajectory, and the trajectory is optimized [14].

These methods all rely on some form of parameterization of the spring characteristic, thereby limiting the set of possible spring characteristics. This effect is exacerbated when the parameters of the spring are optimized numerically. To speed up this optimization, the number of parameters is typically chosen as small as possible, further limiting the set of spring characteristics over which is optimized.

The contribution of this paper is twofold:

1) A method is presented to compute the exact optimal spring characteristic analytically as a function of the trajectory (and dynamics) of systems performing repetitive tasks. This includes rephrasing the trajectory as function of position rather than time. With the analytical optimal spring, the energy consumption of the system reaches its global minimum. The resulting characteristic can be used to fit a mechanical design, or as a benchmark.
2) Two use cases demonstrate the potential value of the method in different applications: a) parallel elastic element design for and active ankle prosthesis, b) design of an extremely energy efficient plugless robot arm.

The example of the ankle prosthesis shows the benefit of the method as an analysis tool. An analytical optimal spring is fitted to data of the human ankle during normal gait. The spring found this way could aid the motor in an active ankle prosthesis. When a parameterization is required to realize the spring characteristic, the shape of the optimal spring characteristic is a useful basis on which to choose an effective parameterization. Comparing different parallel springs, it is shown that a relatively low order piecewise polynomial spring fit to the optimal nonlinear characteristic, outperforms much higher order continuous polynomial springs which were optimized without knowledge of the optimal torque characteristic. Also the manufacturability of nonlinear springs is discussed.

The example of the plugless arm considers the simplified single degree of freedom model shown in Fig. 1b. The method is applied to obtain extreme energy frugality so that the arm can indeed be powered fully by the pick-and-place task it performs. Because the optimal trajectories of the robot depend on the spring characteristic, the spring and trajectories should be optimized simultaneously. In earlier work, both the spring characteristic and the trajectory were parametrized and then optimized numerically [15]. The resulting, non-convex optimization problem proved too large to solve reliably. In this work, we successfully optimize the trajectory by relying on our novel method to optimize the spring characteristic. Comparison with a linear spring shows the optimal spring reduces the energy consumption by 60%, showing the potential benefit of our method. The plugless arm example also shows that the method can be adjusted to more realistic, and hence more complex, loss models.

The remainder of this paper is structured as follows. Our approach is explained in Section II. Subsequently the effectiveness of the method is demonstrated in two different examples of application in Sections III and IV. Sections V and VI provide discussion and conclusion respectively.

II. Method

In this section, we derive the optimal characteristic for a spring used in a parallel elastic actuator that tracks a predefined cyclical trajectory with known external forces.

Trajectories are typically described as functions of time, because time always progresses monotonically. However the spring characteristic is naturally a function of position. Therefore we propose to describe the trajectory also as function of position. We show that with position as independent variable, the optimal spring characteristic no longer needs parameterization and can be described as an analytical function of the trajectory.

The aim is to find the spring characteristic $T_s(\phi)$ optimizing the electric energy consumption of the actuator, E, given a prescribed trajectory as specified by its velocity $\dot{\phi}(\phi)$ and joint torques $T_j(\phi)$ as a function of the position ϕ:

$$T_s^* = \arg\min_{T_s} E \ . \tag{1}$$

The energy consumption is often computed as the integral of power, P, over time. Now we rewrite it as an integral over position, substituting $dt = \dot{\phi}^{-1} d\phi$. This requires that the position is an invertible function of time, i.e., the velocity must not become zero. To allow for more complex cycles, e.g., the ankle prosthesis case, the integral is split in N phases, for which the position over time function is invertible:

$$E = \sum_{i=1}^{N} \int_{\phi_{i,o}}^{\phi_{i,e}} \frac{P_i}{\dot{\phi}_i} d\phi_i \ , \tag{2}$$

where the subscripts i indicate the phases of the motion and o and e indicate the origin and end positions of the phase. At the end of this section, we discuss how a small minimum velocity ϵ is used to avoid the singularity when $\dot{\phi} = 0$.

As the cyclical trajectory and resulting torques are known, the energy consumed as mechanical work is fixed. Therefore we only need to consider electric losses. The electrical power (heat) loss is given as: $P_{\text{heat}} = I^2 R$ where I is the current through the actuator, and R is the resistance of the motor. Furthermore, the motor torque, $T_m = k_m I$, with k_m the motor torque constant. Combining the two equations, we obtain: $P_{\text{heat}} = R k_m^{-2} T_m^2 = \frac{1}{2} c T_m^2$, with the constant c a shorthand, as defined in the equation.

Because the (known) joint torque is provided by the motor and the spring, the motor torque is the difference: $T_{\text{m}} = T_{\text{j}} -$

$T_\mathrm{s}(\phi)$. With the joint torques T_j also a function of position, the electric energy loss is quadratic in the spring torque:

$$E = \sum_i \int_{\phi_{i,o}}^{\phi_{i,e}} \frac{1}{2} c \frac{\left(T_{\mathrm{j},i}(\phi_i) - T_\mathrm{s}(\phi_i)\right)^2}{\dot{\phi}_i(\phi_i)} d\phi_i \ . \tag{3}$$

In the remainder of this paper the function dependence on position ϕ_i is dropped in equations for readability.

Now, to optimize the spring characteristic, we use a classic result from the calculus of variations: the Lagrange equation, see [16] for a derivation. Consider the functional $\mathcal{J}$:

$$\mathcal{J} = \int_{\alpha_0}^{\alpha_1} \mathcal{F}(\alpha, \mathbf{x}(\alpha), \mathbf{x}'(\alpha)) d\alpha$$

for a given integrand $\mathcal{F}$, functions $\mathbf{x}$ to optimize, and independent variable α. The Lagrange equation is a necessary condition for $\mathbf{x}$ to be an optimum of $\mathcal{J}$. It says:

$$\frac{\partial \mathcal{F}}{\partial \mathbf{x}} - \frac{d}{d\alpha} \frac{\partial \mathcal{F}}{\partial \mathbf{x}'} = 0 \ . \tag{4}$$

When applying (4) to the problem of optimizing springs, the angle ϕ is the independent variable, T_s is the function to be optimized and the electric energy loss takes the role of the functional $\mathcal{J}$. Care must be taken to combine the phases of the motion to obtain the integrand $\mathcal{F}$. Since cyclic motion is considered, for every distance $[\phi_{i,a}, \phi_{i,b}]$ traveled one way by trajectory i there is a trajectory j traveling in the opposite direction. Denoting all trajectories from ϕ_{i,a_k} to ϕ_{i,b_k} by odd i and all trajectories from ϕ_{i,b_k} back to ϕ_{i,a_k} by even i, the sum in (3) can be taken into the integral, even when not all i are defined for the full domain $[\phi_{i,o}, \phi_{i,e}]$:

$$\mathcal{F}(\phi, T_\mathrm{s}(\phi)) = \sum_{i_\mathrm{odd}} \frac{1}{2} c \frac{\left(T_{\mathrm{j},i} - T_\mathrm{s}\right)^2}{\dot{\phi}_i} - \sum_{i_\mathrm{even}} \frac{1}{2} c \frac{\left(T_{\mathrm{j},i} - T_\mathrm{s}\right)^2}{\dot{\phi}_i} \ .$$

The minus sign for the second term reflects the opposite sign of the direction of integration in the odd phases. To allow for phases that do not visit the complete domain of the motion, the integrand is taken to be 0 at unvisited positions.

The integrand $\mathcal{F}$ does not depend on $T_\mathrm{s}'(\phi)$, which is the derivative of $T_\mathrm{s}(\phi)$ with respect to ϕ. Therefore (4) says that the optimal spring characteristic function is obtained by solving $\frac{d\mathcal{F}}{dT_\mathrm{s}} = 0$:

$$T_\mathrm{s}\left(T_{\mathrm{j},1}, \dot{\phi}_1, \ldots, T_{\mathrm{j},N}, \dot{\phi}_N\right) = \frac{\sum_i \left((-1)^i T_{\mathrm{j},i} \dot{\phi}_i^{-1}\right)}{\sum_i \left((-1)^i \dot{\phi}_i^{-1}\right)} \ , \tag{5}$$

where the effects of the *even* and *odd* phases are summarized using powers of -1. Since $\dot{\phi}_{i_{odd}}$ are per definition of opposite sign with respect to $\dot{\phi}_{i_{even}}$, the optimal spring profile is the average of the different torque profiles weighted by the inverse of the velocity profiles. Intuitively this can be understood as: the longer an angle is maintained, the more important it is for the spring to match the torque and relieve the motor. In the special case that the torque demands for a given position are the same for all phases, this equation would set the spring torque to this (inverse dynamics) torque. The result is independent of the actuator constants in c.

The solution is singular when $\dot{\phi}_i(\phi) = 0$. This singularity is caused by the indeterminate amount of time spent in a position with zero velocity. The optimum in a singular position would be the joint torque as required by the singular phase, which would cause discontinuities in the spring characteristic. In practice these discontinuities are avoided by introducing a small minimum absolute velocity, $\dot{\phi} = \mathrm{sign}(\dot{\phi})\max(|\dot{\phi}|, \epsilon)$. This ϵ should be chosen small enough that it only gets triggered at the singularities, where it will make the spring characteristic computable. For such a small ϵ the computed spring torque at those points will still heavily weigh towards the torque of the trajectory that is singular at that point, as is the case for the optimal spring torque.

III. Application I: Ankle Prosthesis

In this section, we compute the optimal spring characteristic for a human ankle joint when walking, based on the data by [13]. The complexity of the ankle movement allows us to demonstrate the power of Eq. (5).

The use of elastic elements in ankle orthoses and prostheses has been extensively studied, both for passive [13], [17] and active [18]–[20] devices. These devices aim at improving the walking performance, such as metabolic cost or mechanical power, of the wearer. For such devices, minimizing motor energy can be a factor in the design, as it would lead to smaller motors and longer battery life.

Note that the current method does not consider the use of clutches and dampers, which have been shown to increase the effectiveness of parallel springs in prosthetics [17]. In the future the method may be extended to include these.

Prosthetic and orthotic devices need to account for many factors, including the variability of walking between persons and the extend to which people adapt to the device [21], as well as the reflected inertia induced by the device [22]. The results presented here do not consider those factors, as they solely focus on minimizing the energy losses of an electric motor that replicates the ankle trajectory and torques found in average human walking. Consideration of reflected inertia will shift the exact outcome as presented in this section, yet the results remain illustrative to the problem. As such, these results might be an inspiration for the design of elastic elements of active prostheses.

The data provide average angles, angular velocities and torques of the ankle joint observed during human gait [13]. Time is normalized and the data is provided at a 2% gait cycle-time interval. The data is interpolated by a cubic spline to obtain intermediate values at specific angles, such that the data can be used as a function of position. The data points and the interpolated target trajectory are shown in Fig. 2.

Whenever the direction of movement is reversed, i.e., the angular velocity is zero, the trajectory is split. Four phases are obtained, as shown in Fig. 2. Subsequently the optimal torque characteristic is obtained using (5).

To compare the efficacy of our method to optimizing a parameterized spring, we also compute optimal coefficients, a_i, for a spring characteristic parametrized as polynomial: $T_\mathrm{s} = a_k\phi^k + a_{k-1}\phi^{k-1} + \ldots + a_1\phi + a_0$. The optimal

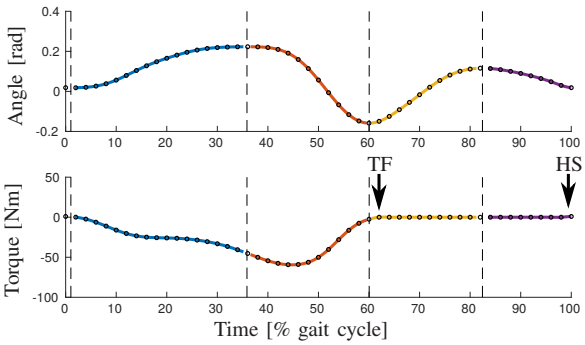

Fig. 2: Ankle angle and torque data interpolated and divided in four phases, "TF", "HS" denoting toe-off and heel-strike.

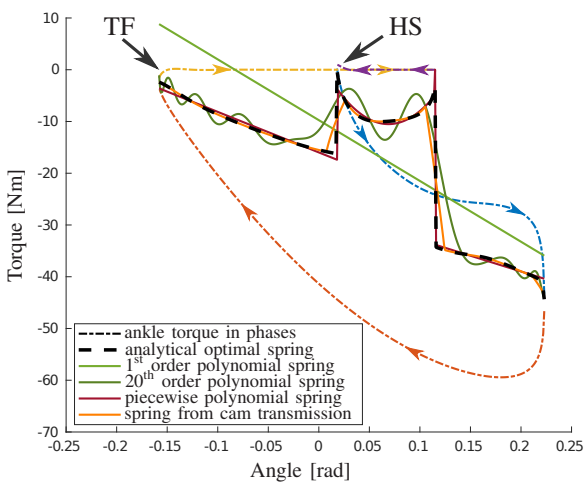

Fig. 3: Torque characteristics of the parallel springs optimized for the ankle data. Also shown is the joint torque required during each phase of the motion. The color coding for these phases is the same as in Fig. 2. "TF" and "HS" denote toe-off and heel-strike respectively.

coefficients can be computed analytically because the cost is quadratic in the coefficients.

A. Results

Figure 3 shows the four phases with torque as a function of position. In the figure, the optimal spring characteristic is shown for the unparameterized optimization and for a low (1st) and a high (20th) order polynomial parameterization. The characteristic of the higher order polynomial approaches the analytical optimal characteristic.

For the unparameterized spring, large jumps in the torque are observed at the angles where a pair of phases starts or ends. Towards the turn of a phase the velocity approaches zero, meaning the weight factor of that phase approaches infinity at those positions. As a result, the spring characteristic is forced towards the torque of that phase. Immediately outside the domain of that phase, the optimal spring torque drops back to the weighted average of the remaining phases, which leads to the large discontinuities observed.

At angles between approximately 0 and 0.1 rad, there is an additional phase at zero torque, representing the relaxation of

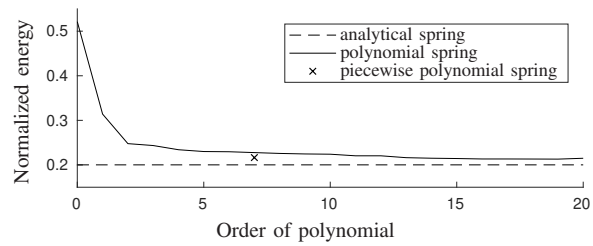

Fig. 4: Electric energy loss for parallel springs parametrized as polynomials, expressed as a fraction compared to actuation without a parallel elastic element. The energy loss of the analytically optimal spring is shown as comparison.

the ankle between mid-swing and heel-strike. This additional zero torque phase causes the optimal spring torque to be lower within that range. The effect is amplified by the fact that this phase has the lowest velocity during that interval.

The normalized electric energy loss for the different parallel springs is shown in Fig. 4. The low energy consumption of the analytical spring is approached by the polynomial spring as the order increases.

Even if the unparameterized spring characteristic is too complicated to design, it does provide valuable insights into the desired characteristic. For instance, the characteristic in Fig. 3 is intuitively well approximated by a piecewise polynomial function. The figure also shows the characteristic of a spring obtained by fitting a piecewise function, with two affine parts and one (middle) quadratic part, to the optimal characteristic. Fig. 4 shows the energy cost of this piecewise polynomial spring, compared to a continuous polynomial with the same number of parameters.

B. Notes towards realization

This section discusses the use of the computed optimal spring characteristics for mechanical design. In general, the optimal characteristic will serve as inspiration or benchmark for designing mechanisms with simple components, such as the pulley system in [3]. It is also possible to approximate the optimal characteristic with a cam mechanism, as we will explore for the spring characteristic computed in Sec. III-A.

To realize a non-linear spring characteristic, we adapt the cam mechanism used in [23]. The shape of the cam is computed using the method in [24]. To smoothen the cam design, the spring characteristic is divided between two parts of the cam surfaces, each followed by a different follower. Figs. 5b-c show a cam design with the same relative sizes as in the original mechanism and a transmission ratio of 4:1. The design can be scaled without changing the shape of the spring characteristic.

A realizable cam shape cannot follow the desired characteristic exactly. Fig. 5a highlights an impossibility due to largest jump in the characteristic. The exact cam shape would require the cam follower to jump between positions, which is not possible in practice. Therefore, the cam is smoothened, using a moving average filter. The corresponding spring characteristic is shown in Fig. 3.

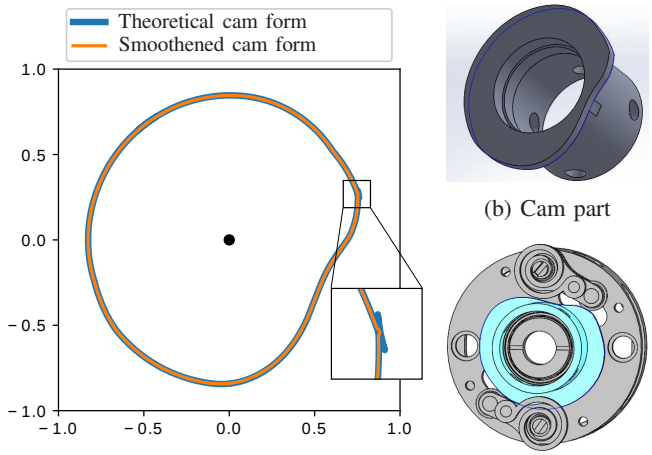

(a) Cam form (b) Cam part (c) Cam in assembly

Fig. 5: Cam design for nonlinear spring transmission

Outside the jumps, the cam characteristic matches the optimal characteristic closely. With this smoothened cam form, the electric energy loss rises from 20.0 % to 21.8 % of the energy that would be lost without parallel spring. There are two main issues that would reduce the energy gain of the mechanism in practice. First are the losses due to friction, which can only be minimized, not avoided, by using low-friction bearings. Second are the imperfections in the manufactured cam shape, which cause a deviation from the expected spring characteristic. The spring stiffness, transmission ratio and size of the cam must be tuned emperically to minimize these two losses and ensure realisability.

The challenges involved in realizing the optimal spring characteristic for this case study are general to most applications. The optimal spring torque will be piecewise continuous, except when all phases cover the full domain of the motion and the desired joint torque is continuous. Section V contains a discussion on how to deal with the discontinuities in the characteristic.

IV. Application II: Pick-and-Place Robot Arm

This section considers a simplified model of the plugless pick-and-place robot, see Fig. 1b. The gripper, mounted on a spindle, receives packages of 1 kg at a height of 1 m, deposits them at ground level and returns without package. This example demonstrates the power of (5) as part of an optimization problem, and shows how that equation can be adjusted to a more complex model. With the analytical optimal spring, the small difference in potential energy is sufficient to power the entire arm, including overhead processes. No additional external energy source is required.

A. System model

This section describes the model for the robot, with the parameter values listed in Table I. The model assumes that the centers of mass of the package, the gripper and the slider coincide. The slider is the spindle nut, which is centered around the spindle shaft through which the motion is actuated. So the acceleration of the combined mass, $\ddot{y}$ is

TABLE I: Model parameters

Gravitational acceleration g	9.81	m/s^2
Mass of package m_{package}	1.0	kg
Mass of gripper m_{gripper}	0.20	kg
Mass of spindle nut m_{slider}	0.65	kg
Spindle reduction ratio n_{s}	157	rad/m
Spindle inertia J_{s}	519	kgmm^2
Forward efficiency η_{p}	0.89	
Backward efficiency η'_{p}	0.87	
Coulomb friction coefficient μ_{C}	0.2	Nm
Viscous friction coefficient μ_{v}	0.05	Nms/rad
Rotor inertia J_{m}	306	kgmm^2
No load current I_{noLoad}	0.538	A
Torque constant k_{t}	71.1	mNm/A
Terminal resistance R	0.343	Ω

$$\left(m + (J_{\text{m}} + J_{\text{s}})n_{\text{s}}^2\right)\ddot{y} = -mg + F_{\text{s}} + Cn_{\text{s}}T_{\text{m}} - F_{\text{f}} \ ,$$

$$m = \begin{cases} m_{\text{slider}} + m_{\text{gripper}} + m_{\text{package}} & \text{when going down} \\ m_{\text{slider}} + m_{\text{gripper}} & \text{when going up} \end{cases} .$$

The dependencies on y have been suppressed for readability, they are stated below. The motor and spindle have inertia J_{m} and J_{s} respectively and the spindle has a transmission ratio n_{s}, resulting in a reflected inertia term $(J_{\text{m}} + J_{\text{s}})n_{\text{s}}^2$. The combined mass m is acted upon by gravity g, spring force $F_{\text{s}}(y)$ as function of position y, and the actuator, of which the torque T_{m} is transformed to a force by the spindle. The main friction acting on the spindle is a nonlinear efficiency C, expressing the torque dependent losses in the transmission:

$$C = \begin{cases} \eta_{\text{p}} & \text{when } \sigma(T_m) = \sigma(\dot{y}) \text{ i.e. accelerating} \\ 1/\eta'_{\text{p}} & \text{when } \sigma(T_m) \neq \sigma(\dot{y}) \text{ i.e. decelerating} \end{cases} , \quad (6)$$

where $\sigma(\cdot)$ denotes the sign function. Additional friction $F_{\text{f}} = \mu_{\text{C}}\sigma(\dot{y}) + \mu_{\text{v}}\dot{y}$ is modeled as a sum of Coulomb friction and viscous friction. The coefficients are estimated based on [25]. Further details about the modeling can be found in [26].

The system equations as function of position are:

$$\frac{d}{dy}\begin{bmatrix} \dot{y} \\ t \end{bmatrix} = \frac{dt}{dy}\begin{bmatrix} \ddot{y} \\ 1 \end{bmatrix} = \dot{y}^{-1}\begin{bmatrix} \frac{-mg - F_{\text{f}} + F_{\text{j}}}{\tilde{m}} \\ 1 \end{bmatrix} ,$$

with an effective mass $\tilde{m} = m + (J_{\text{m}} + J_{\text{s}})n_{\text{s}}^2$, and a combined joint force $F_{\text{j}} = F_{\text{s}} + Cn_{\text{s}}T_{\text{m}}$.

The electric motor model specifies the current, I, and voltage U provided. It relates these to the motor torque T_{m}, the motor torque constant k_{t}, a lost current due to Coulomb friction (I_{noLoad}), and a terminal resistance R:

$$I = I_{\text{noLoad}}\sigma(T_{\text{m}}) + \frac{T_{\text{m}}}{k_{\text{t}}} \ , \qquad U = IR + k_t n_s \dot{y} \ .$$

B. Optimal spring torque

This section applies the method described in Sec. II to the model presented in Sec. IV-A. Here, the energy cost is

$$E = \int \left[T_{\text{m}}n_{\text{s}} + \frac{I^2 R}{\dot{y}}\right] dy + P_{\text{oh}}t_{end} \quad (7)$$

where in integral term is the equivalent of (2) with the electric power $P_{\text{el}} = UI$ divided by velocity $\dot{y}$ integrated over

position y. This first term contains the recovered mechanical energy and the actuator heating. The constant power term outside the integral represents overhead power consumption, a simple model for the energy consumed by the processor, sensors and end-effector [27]. The overhead, estimated to be 4 W [26], affects the duration of the optimized trajectory.

In order to compute the optimal spring force, F_s, following the method presented in Sec. II, the rotational quantities (such as torque) are substituted by their translational counterparts (force). Furthermore, in contrast to the model presented in Sec. II, this model contains terms that depend nonlinearly on T_m and therefore requires (5) to be adjusted.

In our model there are two such terms: the spindle efficiency and the no-load current. Both terms are piecewise continuous, which makes finding the optimal value of the spring force a two step approach. The first step is to find the optimal value within the differentiable domains, using an adjusted version of (5). The second step is to check if the minimum is at any of the points of non-differentiability.

Minimizing (7), the optimal spring force becomes:

$$F_\mathrm{s} = \frac{\sum_i (-1)^i \left(\frac{F_{\mathrm{j},i}}{C_i^2 \dot{y}_i} + \beta I_\mathrm{noLoad} \frac{\sigma(T_{\mathrm{m},i})}{C_i \dot{y}_i} - \frac{1}{\alpha C_i} \right)}{\sum_i (-1)^i \left(C_i^2 \dot{y}_i \right)^{-1}} \ , \quad (8)$$

with $\alpha = \frac{-2R}{k_\mathrm{t}^2 n_\mathrm{s}^2}$ and $\beta = k_\mathrm{t} n_\mathrm{s}$. In the numerator, the first term originates from the electrical energy loss as before, the second term is due to the no-load current and the final term is a mechanical energy loss term due to C not being constant.

The right hand side of (8) is still a function of F_s due to the sign term $\sigma(T_{\mathrm{m},i})$, which is present in C_i (6) as well. Because the cycle consists of only two phases, we can remove these dependencies as follows. Based on (5), we assume that the optimal spring torque lies between the required joint torques of the two phases. The sign of the motor torque follows from the difference between the required joint torques. Furthermore, because $\sigma(\dot{y}_1) = -\sigma(\dot{y}_2)$, we know $C_1 = C_2 = C$ at every position. Implementing this knowledge reduces (8) to

$$F_\mathrm{s} = \frac{\sum_i (-1)^i \left(F_{\mathrm{j},i} \dot{y}_i^{-1} + \beta I_\mathrm{noLoad} C \sigma(T_{\mathrm{m},i}) \dot{y}_i^{-1} \right)}{\sum_i (-1)^i \dot{y}_i^{-1}} \ ,$$

which is similar to (5) except for the second term in the numerator, which biases the weighted average of the joint forces. This no-load current term has the same sign in both phases, due to the power of -1 compensating for the sign change of the motor torque.

Due to the non-differentiability of the no-load current, there are now two alternative values for F_s which may lead to minimal electric power consumption. Each of the choices $F_\mathrm{s} = F_{\mathrm{j},1}, F_\mathrm{s} = F_{\mathrm{j},2}$ causes one of the no load current terms to drop out. The electric energy consumption is checked for the three options of F_s and the optimal spring force is the one resulting in the minimum energy consumption.

C. Trajectory optimization

Now that the optimal spring force is known as a function of the trajectory, only the trajectory of the robot, defining the joint forces F_j required for the task, remains to be optimized.

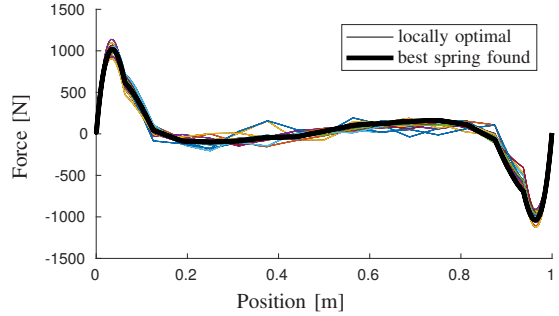

Fig. 6: The 20 springs corresponding to trajectories from the multi-start optimization with the least system energy consumption. The optimal spring of the set is shown bold.

If the path would have been one way, this would have been an inverse dynamics problem parameterized as function of position. However, within a cycle each position is visited multiple times (twice in this case) with different acceleration and friction forces. Therefore we cannot consider it as such.

To allow optimization, the trajectory is parameterized as two piecewise linear functions that set the acceleration divided by the velocity, $\dot{y}^{-1}\ddot{y}$, in the upward and downward motions. For each motion, 16 segments are used. The remaining variables of interest in the optimization are then computed either by direct solution, interpolation, or integration using the 4th order Runge-Kutta algorithm with step size $\Delta y = 1$ mm. At the final positions, $y_{\mathrm{down},N} = 0$ m and $y_{\mathrm{up},N} = 1$ m, both acceleration and velocity are constrained to zero. When integrating the motion, the velocity is constrained to a minimal magnitude of $\epsilon = 1$ mm/s, by clipping both velocity and acceleration.

The optimization is performed using the general purpose interior point method, as implemented by MATLAB `fmincon`. Due to the non-convexity of the problem, we optimize with a multi-start, with 25000 randomly initialized iterations yielding 1347 feasible solutions.

D. Results

Figure 6 shows 20 spring characteristics, corresponding to the 20 different seeds in the optimization that were found to recover most energy. Of the set, the spring characteristic recovering most energy is shown in black. The other, near optimal spring characteristics are all similar to this found optimum, supporting that the found optimum is likely to be very close to the global optimum for the Plugless arm case.

Figure 7 shows the trajectory information corresponding to the optimal spring characteristic. Note that the middle and right plots have double y axes. The joint forces of the up and down motion lie very close together, thereby effectively approaching an inverse dynamics solution to the optimization problem. As the joint forces are the bounds on the optimal spring force (see Sec. IV-B), they nearly overlap it.

Table II compares the robot with optimized spring to actuation with a linear spring and without spring. The linear spring is chosen such that the loaded arm is balanced in the bottom position and the unloaded arm is balanced in

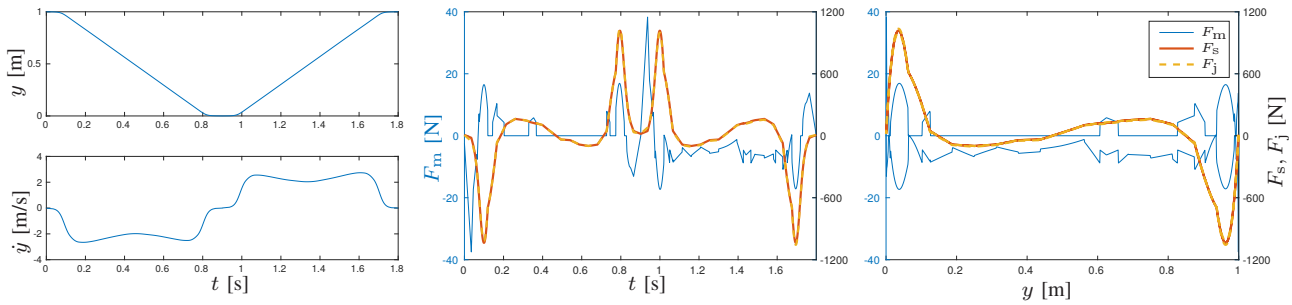

Fig. 7: Optimized trajectory, spring and residual motor torque. The left plots show the position and the velocity as function of time. The middle and right plots show the joint forces and optimal spring characteristic on the right axis, and the motor force on the left axis, plotted over time and position respectively. The motor force is the motor torque scaled by n_s.

TABLE II: Energy measures of the optimal trajectories

units per cycle	net energy	cycle time	mech. loss	I^2R loss	recovered energy
with optimal spring	-0.06 J	1.80 s	1.90 J	0.65 J	7.26 J
with linear spring	14.78 J	4.17 s	2.60 J	5.31 J	1.90 J
without spring	20.36 J	4.00 s	4.44 J	9.71 J	-4.34 J

the top position. This minimizes the power consumption at the standstill positions, as suggested by (5). The supplied potential energy minus the total required energy, E from (7), is denoted as the net energy. The mechanical loss is the difference between the mechanical energy, $\int T_\mathrm{m} n_\mathrm{s} ds$, and the supplied potential energy (9.81 J/cycle). This is the energy lost due to transmission inefficiency. Finally, the recovered energy is the total energy loss without the overhead energy consumption. The number here is the maximum energy available to power on-board systems for a plugless arm. It is seen that without a parallel spring it is not possible to recover energy, even without overheads. With the optimal parallel spring the net energy is negative, meaning that more energy is recovered than required to keep the system running and the arm can function pluglessly.

With the optimal parallel spring, larger overall joint torques are achieved with a fraction of the mechanical and actuator losses. By reducing actuator torques, the spring has reduced the mechanical loss by almost a factor 3 and the I^2R loss by a factor 14. The linear spring shows significantly smaller loss reductions, especially for the I^2R loss. The optimal spring characteristic reduces the total energy consumption of the system by 60% compared to the linear spring. Mechanical heating dominates actuator loss with the optimal spring; the reverse is true for the two other cases.

The remaining mechanical losses originate partially from the transmission efficiency, including Coulomb and viscous friction terms. A less direct mechanical loss factor is the drive train reflected inertia, which increases the effective mass to be accelerated. For the spindle drive used in this model, the reflected inertia is much larger than it will be in an arm with rotational joints, due to adding the significant inertia of the spindle shaft to that of the motor, and due to the relatively large reduction ratio applied to that combined inertia.

V. Discussion

The first part of this discussion covers the method for computing the optimal spring, focussing on extensions in future work; the second part treats the plugless arm use case.

A. Optimal spring characteristic

In this paper we have shown that the nonlinear spring characteristic for a parallel elastic actuator can be optimized analytically if the trajectory and force requirements are known. The resulting spring characteristic is useful as inspiration and benchmark for designing and optimizing mechanisms for parallel elastic actuators.

The main challenge is found in motions in which the direction of movement is reversed multiple times and at different positions, causing the optimal spring characteristic to contain jumps. These jumps occur for the ankle spring in Sec. III. In Sec. III-B, the optimal spring characteristic was smoothened to obtain a realizable characteristic. Future work could investigate how to add smoothness, and other traits of realizable springs, directly in the cost function. This likely requires the optimal spring to be computed numerically.

Alternatively, future research could investigate clutches to either realize or avoid jumps. In particular, concepts like the series-parallel elastic actuator [28] could be used to realize discontinuities. To avoid the discontinuities, clutches could be used to create different spring torques at the same position of the joint, thereby removing the jumps in the optimal characteristic(s). This has proven to be useful if the torque requirements vary between the back and the forth motion, for instance in the case for the ankle motion in human walking [17], [29]. This can also be seen in Fig. 2, which shows a difference in joint torques between the swing and stance phases. Disconnecting the parallel spring during swing will allow the spring to contribute more during stance.

B. Plugless arm

By combining the spring characteristic optimization with a trajectory optimization, we show simulations of a plugless robot performing the pick-and-place task in Fig. 1b. In order to turn this simulation into a robot design, further research into the following issues is necessary.

First, in this paper we optimize for net energy per cycle. For the plugless-arm task, it is sensible to also consider other

goals, such as energy recovery per time (power) and stability. If the motion is quicker, the energy of new packages is injected in the system at a faster rate, hence more power is available for recovery. This can allow for higher overhead or control costs. The power can be optimized within our framework by computing the optimal spring and trajectory for various values of the overhead cost, P_{oh}, and computing the resulting recovered power. In a real world setting, disturbances necessitate control actions to stabilize the robot. By optimizing the spring characteristic to provide a stabilizing effect, the required control torques would be reduced.

Second, the paper discusses a single degree of freedom robot. In order to apply these techniques in an industrial setting, they should handle multi-degree of freedom robots and multiple pick-and-place positions. As the results in this paper rely on integration over a single position, incorporating the positions of multiple joints is an important theoretical challenge. The ideas behind transverse coordinates, as used for control for a walking motion in [30], could possibly be used to accomplish this.

VI. Conclusion

In this paper we have shown that the spring torque that minimizes the motor losses of an electric parallel elastic actuator can be found analytically. The optimal spring torque at a given position is the weighted average of the joint torques required over the occasions when that position is passed, with the inverses of the velocities as weights.

As an illustrating example, the optimal spring characteristic for a human ankle joint during walking was computed. The resulting characteristic and the method used to compute it can be adapted for future prosthetic and orthotic devices.

Finally, we have computed an optimal parallel elastic actuator for a linear robot performing a pick-and-place task. The results show that the optimal characteristic allows the robot to be built pluglessly, i.e., it can restore the energy released by a height drop of the package such that it could function without external electric energy supply. The principles behind this parallel elastic actuator will be used in a future multi-degree of freedom plugless robot arm.

References

[1] S. Seok, A. Wang, M. Chuah, *et al.*, "Design principles for energy-efficient legged locomotion and implementation on the mit cheetah robot," *IEEE/ASME Transactions on Mechatronics*, vol. 20, no. 3, pp. 1117–1129, 2015.

[2] S. Toxiri, A. Calanca, J. Ortiz, *et al.*, "A parallel-elastic actuator for a torque-controlled back-support exoskeleton," *IEEE Robotics and Automation Letters*, vol. 3, no. 1, pp. 492–499, 2018.

[3] M. Plooij and M. Wisse, "A novel spring mechanism to reduce energy consumption of robotic arms," in *IEEE/RSJ Int. Conf. on Intelligent Robots and Systems)*, 2012.

[4] M. Vermeulen and M. Wisse, "Intrinsically safe robot arm: Adjustable static balancing and low power actuation," *International Journal of Social Robotics*, vol. 2, no. 3, pp. 275–288, 2010.

[5] W. Roozing, Z. Li, D. Caldwell, and N. Tsagarakis, "Design optimisation and control of compliant actuation arrangements in articulated robots for improved energy efficiency," *IEEE Robotics and Automation Letters*, vol. 1, no. 2, pp. 1110–1117, 2016.

[6] J. Herder, "Energy-free systems: Theory, conception, and design of statically balanced spring mechanisms," Ph.D. dissertation, Delft University of Technology, 2001.

[7] J. Whitney and J. Hodgins, "A passively safe and gravity-counterbalanced anthropomorphic robot arm," in *IEEE Int. Conf. on Robotics and Automation*, 2014.

[8] U. Mettin, P. X. La Hera, L. Freidovich, and A. S. Shiriaev, "Parallel elastic actuators as a control tool for preplanned trajectories of underactuated mechanical systems," *Int. J. of Robotics Research*, vol. 29, no. 9, pp. 1186–1198, 2010.

[9] G. Folkertsma, S. Kim, and S. Stramigioli, "Parallel stiffness in a bounding quadruped with flexible spine," in *IEEE/RSJ Int. Conf. on Intelligent Robots and Systems*, 2012.

[10] A. Mazumdar, S. Spencer, J. Salton, *et al.*, "Using parallel stiffness to achieve improved locomotive efficiency with the sandia steppr robot," in *IEEE Int. Conf. on Robotics and Automation*, 2015.

[11] W. Wolfslag, M. Plooij, W. Caarls, *et al.*, "Dissipatively actuated manipulation," *Control Engineering Practice*, vol. 34, pp. 68–76, 2015.

[12] J. Pen, W. Caarls, M. Wisse, and R. Babuška, "Evolutionary co-optimization of control and system parameters for a resonating robot arm," in *IEEE Int. Conf. on Robotics and Automation*, 2013.

[13] A. Van den Bogert, "Exotendons for assistance of human locomotion," *Biomedical engineering online*, vol. 2, no. 1, p. 17, 2003.

[14] N. Schmit and M. Okada, "Optimal design of nonlinear springs in robot mechanism: simultaneous design of trajectory and spring force profiles," *Advanced Robotics*, vol. 27, no. 1, pp. 33–46, 2013.

[15] R. Vosse, "Plugless robot arm: Energy recuperation using spring mechanisms," Master's thesis, Delft University of Technology, 2016.

[16] D. Naidu, *Optimal control systems*. CRC press, 2002.

[17] S. Collins, M. Wiggin, and G. Sawicki, "Reducing the energy cost of human walking using an unpowered exoskeleton," *Nature*, vol. 522, no. 7555, pp. 212–215, 2015.

[18] A. Esquenazi, M. Talaty, A. Packel, and M. Saulino, "The rewalk powered exoskeleton to restore ambulatory function to individuals with thoracic-level motor-complete spinal cord injury," *American J. of Physical Medicine & Rehabilitation*, vol. 91, no. 11, pp. 911–921, 2012.

[19] T. Yan, M. Cempini, C. M. Oddo, and N. Vitiello, "Review of assistive strategies in powered lower-limb orthoses and exoskeletons," *Robotics and Autonomous Systems*, vol. 64, pp. 120–136, 2015.

[20] L. Flynn, J. Geeroms, R. Jimenez-Fabian, *et al.*, "Ankle–knee prosthesis with active ankle and energy transfer: Development of the cyberlegs alpha-prosthesis," *Robotics and Autonomous Systems*, vol. 73, pp. 4–15, 2015.

[21] J. Selinger, S. OConnor, J. Wong, and J. Donelan, "Humans can continuously optimize energetic cost during walking," *Current Biology*, vol. 25, no. 18, pp. 2452–2456, 2015.

[22] T. Verstraten, J. Geeroms, G. Mathijssen, *et al.*, "Optimizing the power and energy consumption of powered prosthetic ankles with series and parallel elasticity," *Mechanism and Machine Theory*, vol. 116, pp. 419–432, 2017.

[23] M. Plooij, T. Van Der Hoeven, G. Dunning, and M. Wisse, "Statically balanced brakes," *Precision Engineering*, vol. 43, pp. 468–478, 2016.

[24] D. Tsay and B. Lin, "Profile determination of planar and spatial cams with cylindrical roller-followers," *J. of Mechanical Engineering Science*, vol. 210, no. 6, pp. 565–574, 1996.

[25] M. Plooij, M. De Vries, W. Wolfslag, and M. Wisse, "Optimization of feedforward controllers to minimize sensitivity to model inaccuracies," in *Intelligent Robots and Systems (IROS), 2013 IEEE/RSJ Int. Conf. on*. IEEE, 2013, pp. 3382–3389.

[26] L. van der Spaa, "System dynamic design and control of the plugless robot arm," Master's thesis, Delft University of Technology, 2017.

[27] P. Bhounsule, A. Ruina, *et al.*, "Cornell ranger: energy-optimal control," *Dynamic Walking*, 2009.

[28] G. Mathijssen, D. Lefeber, and B. Vanderborght, "Variable recruitment of parallel elastic elements: Series–parallel elastic actuators (spea) with dephased mutilated gears," *IEEE/ASME Transactions on Mechatronics*, vol. 20, no. 2, pp. 594–602, 2015.

[29] D. Häufle, M. Taylor, S. Schmitt, and H. Geyer, "A clutched parallel elastic actuator concept: Towards energy efficient powered legs in prosthetics and robotics," in *Biomedical Robotics and Biomechatronics (BioRob)*. IEEE, 2012, pp. 1614–1619.

[30] L. Freidovich, A. Shiriaev, and I. Manchester, "Stability analysis and control design for an underactuated walking robot via computation of a transverse linearization," *IFAC Proc. Vol.*, vol. 41, no. 2, pp. 10 166–10 171, 2008.